

# Microfluidic Prototype of a Lab-on-Chip Device for Lung Cancer Diagnostics

Dalila Vieira, Filipa Mata, Ana Moita and António Moreira  
*IN+, Instituto Superior Tecnico Universidade de Lisboa, Lisbon, Portugal*

**Keywords:** Microfluidic Device, Electrowetting, Biofluid Dynamics, Wettability, Lung Cancer.

**Abstract:** Cell sorting for disease diagnostics is often achieved by fluorescence based identification of specific markers. However, in lung cancer diagnostics, cytological analysis of pleural fluids is not always reliable and immunofluorescence essays demand for specific sample preparation. Hence, this paper addresses the development of a microfluidic device for lung cancer diagnostics which infers on the potential of a diagnosis based on analysing the cell deformability (stiffness) that alters the rheological properties and consequently the flow characteristics. Cell deformability will be induced by external actuation. Electrowetting is used to transport the samples in an open configuration system using microdroplets. Effects of the test chip configuration, sample physico-chemical properties and potential adsorption mechanisms are discussed. Wettability plays here a vital role in the sample transport and in the diagnostic method to be tested. Hence, an innovative approach is presented, the 3D Laser Scanning Fluorescence Confocal Microscopy (3D-LSCFM) to provide a detailed reconstruction of the surface topology at the liquid-solid interface region thus allowing contact angles measurement with high spatial resolution.

## 1 INTRODUCTION

Cell separation and sorting are critical in various biomedical applications including diagnosis, therapeutics and cell biology (Takahashi et al., 2004, Gossett et al., 2010, Shields IV et al., 2011). Samples of interest are often heterogeneous populations of cells in a culture that comprises tissue. For instance, the analysis of pleural fluid for lung cancer diagnosis requires the previous separation of various components, including blood cells (Gossett et al., 2010). Although many standard techniques have been developed for cell sorting, there are still several challenges to overcome: they are often labour intensive, require multiple additional tags or labels to identify cells, have high costs, use large sized equipment with low portability and require highly skilled staff (Omori et al., 2015). Microfluidic devices are pointed to be able to solve many of the aforementioned problems and are actually considered a fundamental pillar for the development of point-of-care diagnostics (Yager et al., 2008). Within this scope, this work aims at devising a microfluidic chip for a lung cancer diagnosis. One explores here the possibility to provide an earlier diagnosis based on the deformability (stiffness) of

the cell, which alters the rheological properties and consequently the flow characteristics. This new approach follows the method suggested by (Gossett et al., 2010), although these authors focused the diagnostics on image analysis of the cells. Instead, here, main emphasis is put on the cell deformation inside microdroplets, as droplet spreading is expected to be correlated to the rheological modifications due to cells stiffness (Moita et al., 2015). Microdroplets are also interesting regarding sample handling in the microfluidic device. Sample transport in continuous medium using microchannels is the most popular approach in microfluidics, but has problems associated with clogging, maintenance and access to the samples. These difficulties can be overcome with an open configuration system, handling the samples in microdroplets, combining an external actuation with custom made wetting properties of the surfaces (Pollack et al., 2011, Moita et al., 2016). However, external actuation (e.g. electrostatic) may influence the internal droplet flow, thus affecting droplet motion (Mugele, 2009). Hence, a complete characterization of the flow is required to tune the appropriate conditions for the transport. Lab-on-a-chip open configuration systems are still sparsely reported in the literature, concerning the transport of biofluids. Several

authors report the effective electrowetting-induced transport of physiological fluids, proteins and DNA (Wheeler et al., 2005), but it is not clear which are the most suitable electrochemical properties of the fluids or the most important parameters governing biofluids transport and manipulation. Adsorption of the biocomponents on the dielectric substrate is also a problem that is not completely understood yet and its effects on the surface wettability are taken to a secondary level. Yoon and Garrell (2003) showed that protein solutions are often adsorbed by the dielectric substrates. Recent work by Moita et al. (2016) evidences that adsorption locally reduces the contact angle, which aids droplet spreading but also promotes energy dissipation at the contact line, thus precluding droplet receding and making the droplet transport more difficult, so this effect should not be neglected. Finally, studies concerning EWOD applications on microchips barely assess the influence of design and configuration parameters. As the droplet is transported on the chip surface, the size and distance between electrodes must account for the wetting properties and how they affect droplet dynamics, which should be balanced by the parameters affecting the electrical field. In this context, for an initial stage of the development of the microfluidic device, an optimization of the chip configuration, taking into account the effect of the liquid and surface properties is required.

Wettability plays a vital role in these flows, but also here improved diagnostic techniques are required to measure the micro-contact angles, which can be significantly different from the apparent angles typically obtained with tensiometers (Sundberg et al., 2007, Vieira et al., 2016). In this context, confocal fluorescence microscopy, which is already used to infer on the potential adsorption mechanisms is further explored here as a new technique providing contact angle measurements with high spatial resolution.

## 2 EXPERIMENTAL PROCEDURE

At this stage of the work, simple microfluidic chips were devised to select the appropriate chip configurations and materials and to infer on the efficacy of the sample transport using electrowetting. Biomimetic solutions of the pleural fluid (as well as pleural fluid) are intended to be used in the near future but for these preliminary tests protein solutions and cell suspensions were used as biofluid samples. GFP – Green Fluorescent Protein (produced and purified in house) solution with

$1.71 \times 10^{-3}$  mM concentration and GFP-expressing *E. coli* suspensions with concentrations of  $1 \times 10^9$  cells/ml and  $2 \times 10^9$  cells/ml were the solutions chosen, whose main physico-chemical properties, namely density  $\rho$ , surface tension  $\sigma_{lv}$  and dynamic viscosity  $\mu$  are summarized in Table 1. Regarding their rheology, all the fluids used here are Newtonian.

Table 1: Physico-chemical properties of the biofluids.

Solution	Density $\rho$ [kg/m <sup>3</sup> ]	Surface tension $\sigma_{lv}$ [mN/m]	Dynamic viscosity $\mu$ [Ns/m <sup>2</sup> ]
GFP ( $1.71 \times 10^{-3}$ mM)	998	72.2±0.7	$1 \times 10^{-3}$
GFP-expressing <i>E. coli</i> ( $1 \times 10^9$ cells/ml)	998	73.8±0.04	$1 \times 10^{-3}$
GFP-expressing <i>E. coli</i> ( $2 \times 10^9$ cells/ml)	998	73.8±0.04	$1 \times 10^{-3}$

For the measurements with the 3D Laser Scanning Fluorescence Confocal Microscopy – 3D LSCFM a fluorescent dye - Rhodamine B (Sigma Aldrich) is used, which was chosen taken into account its excitation and emission wavelengths, to be compatible with the wavelengths available in the Laser Scanning Confocal Microscope (Leica SP8), but also due to particular characteristics of the experimental conditions, in the present study. For the concentrations used here ( $0.0007936 \text{ mg/ml} < \text{Concentration} < 0.496 \text{ mg/ml}$ ) the physico-chemical properties of the water-dye solutions are very close to those of water. Detailed description of the measurement procedures is provided in Vieira et al. (2016).

The test chips, manufactured at INESC-MN are printed by lithography and the patterned transferred by wet etch. Finally, a thin film of a dielectric material is deposited on the chip assembly. The chips mainly comprise numerous interdigitated electrodes displaced with a fixed distance of 60 $\mu\text{m}$  between them. The variable in the chips configuration is the width of the electrodes, which varies between 80 $\mu\text{m}$  and 1400 $\mu\text{m}$ . The length of the electrodes is 24mm. The usable chip area is 32x22mm<sup>2</sup>. The applied voltage is varied from 0 to 250V, also to infer on its influence on the droplet motion. The frequency was varied between 50Hz and 450Hz. To infer on the possible adsorption of the biocomponents on the dielectric substrates over which the droplets of the biofluids are transported, simple tests are performed in which droplets of the biofluids are deposited on the surfaces. Afterwards,

a sequence of tests with and without electrostatic actuation is performed and the “footprints” of the droplets are observed on the Laser Scanning Confocal Microscope (Leica SP8). The obtained images are then post-processed to determine the mean grey intensity (sum of intensities divided by the number of pixels in the region of interest of the droplet footprint) and the Area Integrated Intensity (sum of intensities of pixels in the region of interest of the droplet footprint normalized by unit of area ( $\mu\text{m}^2$ )). Since the droplet spreads after actuation, the integrated density is weighted with the area. To reduce the noise, the average grey intensity levels of the background image were also subtracted. The final result is the herein so-called Total Corrected Droplet Fluorescence – TCDF, as proposed by Moita et al. (2016). Higher values of TCDF can be associated to a larger quantity of the protein or cells adsorbed by the substrate. The wetting properties of the dielectric substrates play a vital role. Different chemical and topographical characteristics are tested to infer on the most favourable to handle the biosamples in the various sections of the microfluidic device. The topography is measured using a Dektak 3 profile meter (Veeco) with a vertical resolution of 20nm.

The wettability of the dielectric substrates is quantified with an optical tensiometer (THETA from Attention), by the static contact angle  $\theta_c$  and by hysteresis. Given the relatively low resolution of these measurements and considering the typical scale of the processes governing the transport of the samples within the droplets (micro-to-nano scale) an alternative method is explored to provide more accurate measurements. Detailed description of this technique can be found in Vieira et al. (2016). Finally, transport and deformation of the biofluid droplets are characterized based on high-speed visualization at 2200 fps using a Phantom v4.2 from Vision Research Inc., with 512x512 pixels@2100fps resolution. Post-processing home-made routines are then used to measure deformability, spreading diameters, velocity of droplets transport and displacement velocity of the contact line (droplet-dielectric substrate).

### 3 DEVICE CONFIGURATION

The microfluidic device under development has three main working sections, namely, the transport section, the diagnostic section and the sorting/selection section. In the transport section, which enables the transport of the biofluid droplet to

the diagnostic section, droplet motion is governed by electrostatic actuation aided by custom made wetting properties of the dielectric material. In this section, hydrophobic/superhydrophobic regions are preferred to minimize the adhesive forces, which are proportional to hysteresis and consequently minimize the energy dissipated at the contact line between the droplet and the surface. Similar wetting properties are required in the sorting/selection section. On the other hand, in the diagnostic section it is worth promoting adhesion to constrain the sample in the sensor area. The diagnostic methodology to explore considers the correlation of different ratios of cell stiffness with the degrees of the pathology, being expected to be able to detect cell malignancy at very early stages (Gosset et al, 2010). The deformation of the cells inside the microdroplets is induced. Different approaches will be explored to impose the deformation but at this stage of the work, electrostatic actuation is being tested. A numerical model is being developed at two scales. At the mesoscale, the deformability of the cell is simulated. At this scale surface wettability effects, such as adhesion and repulsion, are related to molecular bonding and Van de Walls forces. The main outputs of this model are the forces that must be exerted to impose the various degrees of deformability of the cell to validate the diagnostic method. On the other hand, despite being a macroscopic flow, the spreading of a microdroplet is known to be very sensitive to small rheological modifications of the fluid and can be correlated with the parameters governing the constitutive models (Moita et al., 2015). Hence droplet spreading is expected to be correlated to the various levels of cell stiffness. These levels of cell stiffness can be grouped in classes of internal cell viscosity/water viscosity and correlated to different degrees of the pathology. At this scale, surface wettability can simply be modelled based on interfacial tensions, hysteresis and contact angle values, but still requires very accurate contact angle measurements combined with a detailed characterization of the droplet internal flow, particularly near the surface.

Following the discussion in the previous paragraphs, the selection of the materials to use as the dielectric film, plays here a determinant role, as different sections of the microfluidic chip demand for opposite wetting regimes. The first approach considered here was tailoring surface topography to alter the wettability. Hence, photolithography was used to define micro-patterns of regular cavities/pillars. For an accurate measurement of the contact angles and clearer description of the contact

line, the contact angles were with a new technique, the 3D LSCFM, described in the next paragraphs.

### 3.1 Contact Angle Measurements with 3D LSCFM

To validate and explore the 3D LSCFM technique, preliminary results were obtained by measuring the equilibrium contact angles on smooth glass slides. The equilibrium angles are measured for millimetric (with diameters of 3mm) and micrometric (with diameters ranging between tens of microns up to 1mm) droplets, to infer on their dependence on droplet size. The obtained measures are compared with those obtained with the optical tensiometer (Figure 1).

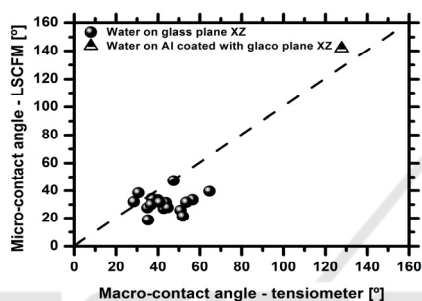


Figure 1: Comparison between the equilibrium angles measured with tensiometer and with the LSCFM technique, measured for a smooth glass and coated Al surfaces.

Overall the results show that both techniques provide similar measurements, although the values obtained from the LSCFM tend to be lower, when compared to those given by the optical tensiometer. This is due to the scale and resolution that are being considered in the LSCFM. Hence, the error associated to the worse resolution used in the LSCFM is of  $1.87\mu\text{m}$  (with negligible propagation to the angle measurement) against  $156\mu\text{m}$  obtained with the optical tensiometer. So a more detailed view of the contact line region can be obtained with the 3D LSCFM, which consequently provides a more accurate shape of the region defining the contact angle. These observations are qualitatively in agreement with those reported by Salim et al. (2008).

Once the measurement technique is validated, it can be applied to more complex surfaces, namely those with patterned micro-structures. For these surfaces a large difference is observed between the measures obtained with the optical tensiometer and those taken with the 3D LSCFM technique, as depicted in Figure 2. Hence, there are apparent

angles of  $120^\circ$ , as measured by the tensiometer, thus evidencing a hydrophobic behavior, which are in fact up to  $40^\circ$  lower, when measured with the 3D LSCFM technique.

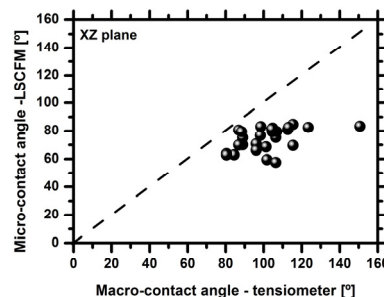


Figure 2: Comparison between the equilibrium angles measured with the optical tensiometer and with the LSCFM technique measured on micro-textured silicon wafer surfaces.

The lower angles measured with the 3D LSCFM are in agreement with the observations of the contact line region. So, the apparent hydrophobic regime of some of the surfaces characterized with the tensiometer is not accurate and often not stable, as the liquid droplet sags in between the surface patterns. Furthermore, the 3D reconstructions of the droplet on both XZ and YZ planes show an evident distortion of the contact line. These observations of the contact line may also support our previous results (e.g. Moita et al 2016) which showed that surface topography in these non-stable hydrophobic surfaces promotes energy dissipation at the contact line, thus precluding droplet motion. In line with these results, the safest way to alter wettability, for the current stage of development of the work is towards the chemical modification and/or selection of the appropriate dielectric materials, as discussed in the following sub-section.

### 3.2 Selection of the Materials as a Function of the Influencing Parameters

The selection of the dielectric materials to use should be based on the contact angle measurements but also on the hysteresis, which should be the smallest possible, since the resistance force opposing to droplet motion is proportional to the surface tension  $\sigma_{lv}$  and to the hysteresis. In this context Table 2 depicts the equilibrium angles, obtained for each biofluid tested, on various dielectric coatings which are commonly used in electrowetting chips. Water is used as reference. The Table shows that only the SU8 resist and  $\text{Si}_3\text{N}_4$  surfaces are

hydrophilic, being the others hydrophobic. The highest contact angle of  $121^\circ$  is obtained for the PDMS substrate. Despite having high contact angles, which is desired for the transport of the samples, PDMS and Teflon substrates depict also high hysteresis (Figure 3).

Table 2: Equilibrium contact angles, obtained for each pair fluid-dielectric substrate considered in the present work.

Dielectric coating	Contact angle [ $^\circ$ ]		
	Water	<i>E-coli</i>	GFP
Teflon	112 $\pm$ 5	103 $\pm$ 6	121 $\pm$ 6
Teflon with Glaco	145 $\pm$ 1	141 $\pm$ 9	153 $\pm$ 3
PDMS	121 $\pm$ 1	112 $\pm$ 1	119.5 $\pm$ 0.4
PDMS with Glaco	153 $\pm$ 3	153 $\pm$ 2	155 $\pm$ 3
SU8 resist	67.1 $\pm$ 0.7	65 $\pm$ 2	71.8 $\pm$ 0.2
SU8 with Glaco	160 $\pm$ 7	162 $\pm$ 1	153 $\pm$ 4
Si <sub>3</sub> N <sub>4</sub>	64.1 $\pm$ 0.7	59 $\pm$ 4	65 $\pm$ 2

Glaco® is a commercial coating which is mainly a perfluoroalkyltrichlorosilane combined with perfluoropolyether carboxylic acid and a fluorinated solvent (Kato et al., 2008). Its application allows obtaining superhydrophobic surfaces with high contact angles ( $>150^\circ$ ) and low hysteresis ( $<10^\circ$ ) being therefore a good option to consider in the transport section of the microfluidic device.

Concerning adsorption, Moita et al. (2016) report that the GFP protein was adsorbed by Teflon substrates, leading to a local increase of surface wettability and further contributing to preclude the receding motion, as this wettability increase is irreversible, taking the contact angles to values near saturation.

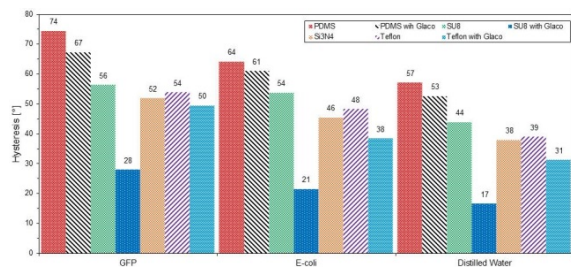


Figure 3: Contact angle hysteresis evaluated for GFP solution ( $1.71 \times 10^{-3}$  mM), GFP-expressing *E-coli* suspension ( $1 \times 10^9$  cells/mL) and distilled water on the tested dielectric substrates.

In this context, this work infers on the possible adsorption of the GFP and *E-coli* cells by the substrates, evaluated by the TCDF value. The results evidenced a minimum value of TCDF =

$8.88 \times 10^7$  and  $TCDF = 1.65 \times 10^7$  obtained for the adsorption of GFP ( $1.71 \times 10^{-3}$  mM) and *E-coli* suspension ( $1 \times 10^9$  cells/mL) on PDMS, respectively. The alternative material with lower adsorption of the biocomponents tested here was SU8, but the TCDF values obtained were about one order of magnitude higher than those evaluated for PDMS. Hence, PDMS is a good choice. In addition, the application of Glaco® coating is observed to further reduce the adsorption of both proteins and cells, decreasing the TCDF values in about one order of magnitude. Once the material is selected, its effect must be further evaluated in the dynamic response of the droplet and its deformability, which also depends on the properties of the biofluids. For illustrative purposes and due to paper length constrains, Figure 4 depicts the effect of the biofluid properties on droplet motion on electrowetting (in the transport section), evaluated based on its maximum spreading diameter, made non-dimensional with the initial droplet diameter as it is collected on the surface,  $d_{max}/d_{0V}$ . The Figure evidences the better response of the droplets of protein solutions, although the surface tension and density only vary slightly between the different solutions (Table 1). Since the cellular compounds are bigger and heavier than the proteins, they should be more difficult to carry. In fact, the cells have a greater propensity to adhere to the surface and tend to agglomerate, increasing the local density and ending up creating resistance to motion. All these aspects must be considered in the following new configurations of the microfluidic chip, once the materials are selected.

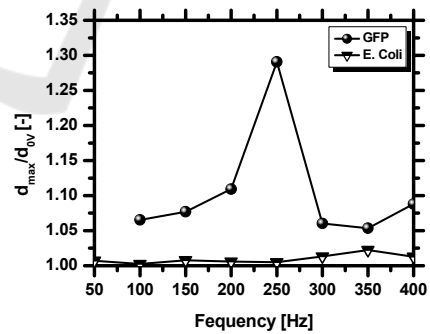


Figure 4: Maximum spreading dimensionless diameter of GFP ( $1.71 \times 10^{-3}$  mM) and GFP-expressing *E-coli* suspension ( $1 \times 10^9$  cells/mL), for droplets moving between coplanar electrodes (transport section of the device).

## 4 SUMMARY

The present paper presents the preliminary stages of development of a microfluidic device for lung

cancer diagnostics which infers on the potential of a diagnosis based on analysing the cell deformability (stiffness). The cell stiffness is expected to alter the rheological properties and consequently the flow characteristics in a detectable way, which is correlated with cell malignancy. The main concepts behind this new diagnostic method are explained together with the global description of the microfluidic device. Given the important role of the wettability, a new methodology is explored here to obtain contact angle measurements with high spatial resolution. At this preliminary stage of the work, the importance of the wettability is discussed in the selection of the materials. The dynamic response of different biofluids is also briefly discussed.

## ACKNOWLEDGEMENTS

The authors are grateful to Fundação para a Ciência e a Tecnologia (FCT) for partially financing this research through the project UID/EEA/50009/2013, which also supports Dalila Vieira with a fellowship. The work was also partially financed by FCT through the project RECI/EMS-SIS/0147/2012, which also supported Filipa Mata with a fellowship. A.S. Moita also acknowledges the contribution of FCT for financing her contract through the IF 2015 recruitment program. Finally, the authors acknowledge the contribution of Joana Pereira in the data acquisition and post-processing of the 3D-LSCFM data.

## REFERENCES

- Gossett, D., Weaver, W., Mach, A., Hur, S., Tse, H., Lee, W., Amini H., Carlo, D., 2010. Label-free cell separation and sorting in microfluidic systems, *Analytical and Bioanalytical Chemistry*, 397:3249-3267.
- Kato M, Tanaka A, Sasagawa M, Adachi H, 2008. Durable automotive windshield coating and the use thereof. US Patent, 8043421 B2.
- Moita, A. S., Laurência, C., Ramos, J.A., Prazeres, D. M. F., Moreira, A. L. N., 2016. Dynamics of droplets of biological fluids on smooth superhydrophobic surfaces under electrostatic actuation, *J. Bionic Eng.*, 13:220-234.
- Mugele, F., 2009. Fundamental challenges in electrowetting: from equilibrium shapes, to contact angle saturation and drop dynamics, *Soft Materials*, 5:3377-3384.
- Omori, T., Imai, Y., Kikuchi, K., Ishikawa, T., Yamaguchi, T., 2015. Hemodynamics in the Microcirculation and Microfluidics, *Annals of Biomedical Engineering*, 43:238-257.
- Pollack, M. G., Pamula, V.K., Srinivasan, V., Eckhardt, A.E., 2011. Applications of electrowetting-based digital microfluidics in clinical diagnostics, *Expert Ver. Molecular Diagnostics*, 11(4):397-407.
- Salim, A., Sausse, J., Pironon, J., Fourar, M., Le Carlier De Veslud, C., 2008. 3D confocal laser microscopy to quantify contact angles in natural oil-water mixtures, *Oil & Gas Sci Tech. Rev. IFP*, 63(5):645-655.
- Shields IV, C. W., Reyes, C. D., López, G. P., 2015. Microfluidic Cell Sorting: A Review of the Advances in the Separation of Cells from Debulking to Rare Cell Isolation, *Lab on a Chip*, 16:1230-1249.
- Sundberg, M., Mansson, A., Tagerud, S., 2007. Contact angle measurements by confocal microscopy for non-destructive microscale surface characterization, *J. Coll. Int. Sci.*, 312:454-460.
- Takahashi, K., Hattori, A., Suzuki, I., Ichiki, T., 2004. Non-destructive on-chip cell sorting system with real-time microscopic image processing, *Journal of Nanobiotechnology*, 2:1-8.
- Vieira, D., Moita, A. S., Moreira, A. L. N., 2016. Non-intrusive wettability characterization on complex surfaces using 3D Laser Scanning Confocal Fluorescence Microscopy, *18th International Symposium on Applications of Laser and Imaging Techniques to Fluid Mechanics*, Lisbon.
- Wheeler A R, Moon H, Kim C J, Loo J A, Garrell R L., 2004. Electrowetting-based microfluidics for analysis of peptides and proteins by matrix-assisted laser desorption/ionization mass spectrometry. *Analytical Chemistry*, 76, 4833-4838.
- Yager, P., Domingo, G., Gerdes, J., 2008. Point-of-care diagnostics for global health, *Annu. Rev. Biomed. Eng.*, 10:231-240.
- Yoon J Y, Garrell R L., 2003. Preventing biomolecular adsorption in electrowetting-based biofluidic chips. *Analytical Chemistry*, 75, 5097-5102.